PROCEEDINGS OF SCIENCE

Production of the hidden charm state $X(3872)$ and of $\psi(2S)$ with the ATLAS detector

James Broughton, on behalf of the ATLAS Collaboration
University of Birmingham (GB)
E-mail: j.broughton@cern.ch

Differential cross sections are presented for the prompt and non-prompt production of the hidden-charm state $X(3872)$ and $\psi(2S)$, in the decay mode $J/\psi\pi^+\pi^-$, measured at $\sqrt{s} = 8$ TeV by the ATLAS detector at LHC. In the non-prompt production, the data suggest the presence of a short-lived component, which may be due to B_c decays. The dipion invariant masses in both $X(3872)$ and $\psi(2S)$ are measured and compared to theoretical predictions.

PoS(DIS2017)125

25th International Workshop on Deep Inelastic Scattering and Related Topics
3-7 April 2017
University of Birmingham, Birmingham, UK

© Copyright owned by the author(s) under the terms of the Creative Commons Attribution-NonCommercial-NoDerivatives 4.0 International License (CC BY-NC-ND 4.0).

1. Introduction

The hidden-charm state $X(3872)$ was discovered by the Belle Collaboration in 2003 through its decay to $J/\psi\pi^+\pi^-$ [1]. Its existence was confirmed soon after by other experiments, including CDF who constrained the possible quantum numbers J^{PC} to be either $J^{PC} = 1^{++}$ or 2^{-+} [2, 3]. LHCb was the first experiment at the LHC to observe the $X(3872)$ [4], which confirmed its quantum numbers to be 1^{++} [5]. The $X(3872)$ has a mass close to the $D^0\bar{D}^{*0}$ threshold and, as a result, the state was initially hypothesised to be a $D^0\bar{D}^{*0}$ molecule with a very small binding energy [6]. CMS performed a cross-section measurement of promptly produced $X(3872)$ [7] as a function of p_T, which showed the non-relativistic QCD (NRQCD) prediction [8] for prompt $X(3872)$ production, assuming a $D^0\bar{D}^{*0}$ molecule, was too high. The current interpretation of the state is a mixed $\chi_{c1}(2P) - D^0\bar{D}^{*0}$ state, where the $X(3872)$ is produced predominantly through its $\chi_{c1}(2P)$ component. CMS data show a good agreement with this new model [9].

The ATLAS collaboration [10] previously reported evidence for the $X(3872)$ state while measuring the cross section of prompt and non-prompt $\psi(2S)$ meson production in the $J/\psi\pi^+\pi^-$ decay channel with 2011 data at $\sqrt{s} = 7$ TeV [11]. ATLAS has performed an extension to this analysis using 11.4 fb^{-1} of $\sqrt{s} = 8$ TeV proton-proton collision data [12].

2. Event Selection

This analysis searches for $X(3872)$ and $\psi(2S)$ decaying to $J/\psi\pi^+\pi^-$, where the J/ψ meson decays into a muon pair. Events used in this analysis are triggered by a pair of muons successfully fitted to a common vertex. Each muon candidate reconstructed offline must have good spatial trigger-object matching that satisfies $\Delta R = \sqrt{(\Delta\phi)^2 + (\Delta\eta)^2} < 0.01$, where ΔR is the angular distance between the momenta of the muon candidate and the trigger object, ϕ is the azimuthal angle around the z-axis and η is the pseudorapidity defined in terms of the polar angle θ as $\eta = -\ln\tan(\theta/2)$. Events where two oppositely-charged muon candidates are reconstructed, with pseudorapidity $|\eta^\mu| < 2.3$ and transverse momenta $p_T^\mu > 4$ GeV, are kept only if the invariant mass of the dimuon system falls within ± 120 MeV of the mass of the J/ψ meson, $m(J/\psi) = 3096.9$ MeV [13]. The dimuon invariant mass is shown in Figure 1(a).

The two muon tracks are fitted to a common vertex with a loose cut on fit quality, $\chi^2 < 200$. The dimuon invariant mass is then constrained to the J/ψ mass, and the four-track vertex fit of the two muon tracks and pairs of opposite-charged non-muon tracks is performed to find the $J/\psi\pi^+\pi^-$ candidates. The two non-muon tracks are assigned pion masses, and are required to satisfy $p_T^\pi > 0.6$ GeV and $|\eta^\pi| < 2.4$. To further suppress the background, the four-track candidates with χ^2 probability $P(\chi^2) < 4\%$ are discarded. The opening angle $\Delta R(J/\psi, \pi^+)$ must be less than 0.5 and the mass difference between the four track candidate and the combination of $m(J/\psi)$ plus $m(\pi^+\pi^-)$ must be less than 300 MeV.

Four-track candidates passing the above selection and lying within the rapidity region $|y| < 0.75$ are used in the analysis. The four-track invariant mass distribution is shown in Figure 1(b). These selection requirements are found to be $> 90\%$ efficient for the $\psi(2S)$ and $X(3872)$ decays in signal Monte-Carlo, while significantly suppressing the combinatorial background.

PoS(DIS2017)125

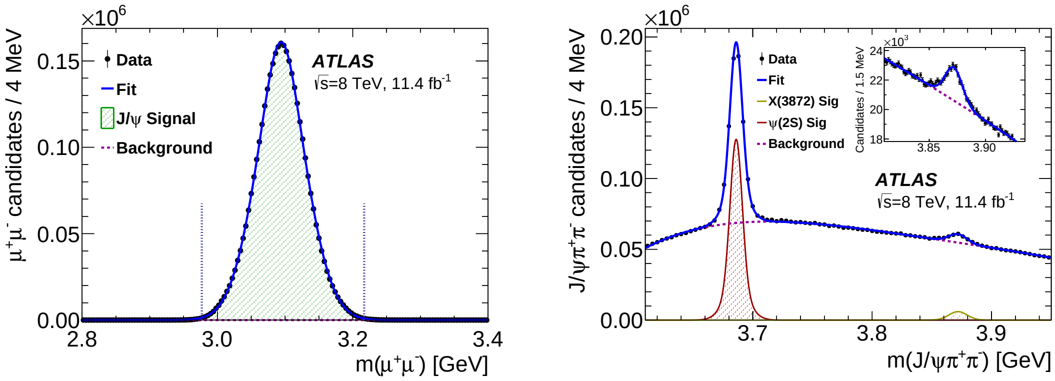

(a) (b)

Figure 1: (a) Invariant mass distribution of the J/ψ candidates satisfying all selection criteria except the J/ψ mass window requirement [12].(b) Invariant mass of the selected $J/\psi\pi^+\pi^-$ candidates after selection requirements [12].

3. Analysis Method

Candidates that pass the selection criteria are weighted based on acceptance, reconstruction and trigger efficiency. Events are divided into five p_T bins and four effective pseudo-proper lifetime τ bins, where $\tau = L_{xy}m/p_T$ with $L_{xy} = \vec{L}\cdot\vec{p}_T/p_T$ and $\vec{L}$ is the vector pointing from the primary pp collision vertex to the $J/\psi\pi^+\pi^-$ vertex. Separation based on the pseudo-proper lifetime distinguishes the prompt production of the $\psi(2S)$ and $X(3872)$ states from the non-prompt production occurring via the decays of long-lived particles such as b-hadrons.

For each p_T and lifetime bin, a minimum χ^2 fit in the $J/\psi\pi^+\pi^-$ invariant mass is performed to determine the signal yields of the $\psi(2S)$ and $X(3872)$ states. For each p_T bin, the yields in individual lifetime windows are fitted separately for $\psi(2S)$ and $X(3872)$.

4. Lifetime Fits

The probability density function (PDF) describing the dependence of $\psi(2S)$ and $X(3872)$ signal yields on the pseudo-proper lifetime τ is a superposition of prompt (P) and non-prompt (NP) components:

$$F^i(\tau) = (1 - f^i_{NP})F^i_P(\tau) + f^i_{NP}F^i_{NP}(\tau), \tag{4.1}$$

where f_{NP} is the non-prompt fraction, while i stands for either $\psi(2S)$ or $X(3872)$ signals. The term f_{NP} is measured in each p_T bin, separately for each i. The prompt signal F^i_P is described by a lifetime resolution function determined from the data. For the non-prompt signal F^i_{NP}, a single one-sided exponential is convolved with the resolution function, with a single "effective pseudo-proper lifetime" fitted to the data. This approach is known as the single-lifetime fit.

Figure 2(a) shows the measured effective pseudo-proper lifetimes τ_{eff} for non-prompt $X(3872)$ and $\psi(2S)$ decays in bins of p_T. While for $\psi(2S)$ the fitted values of τ_{eff} are measured to be around 1.45 ps in all p_T bins, the signal from $X(3872)$ at low p_T tends to have shorter lifetimes, suggesting there could be a different production mechanism contributing at low p_T.

In Figure 2(b) the measured ratio of non-prompt production cross sections of $X(3872)$ and $\psi(2S)$ is plotted as a function of p_T with a kinematic template fitted. The template assumes that

PoS(DIS2017)125

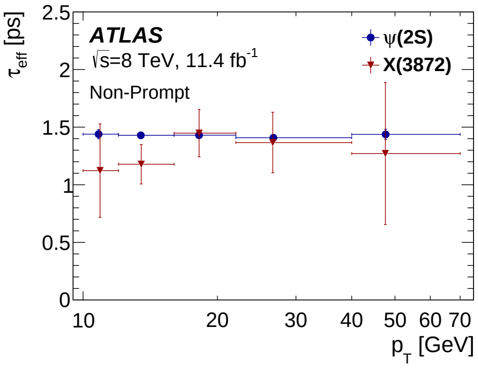

(a)

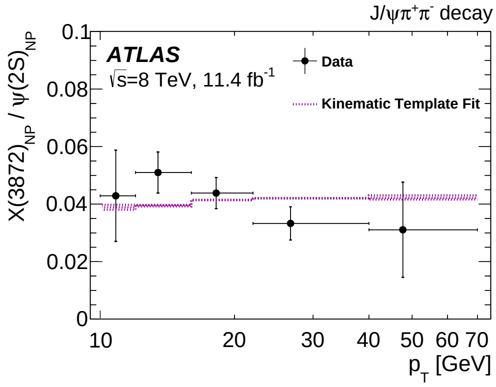

(b)

Figure 2: (a) Measured effective pseudo-proper lifetimes for non-prompt $X(3872)$ and $\psi(2S)$ [12]. (b) Ratio of non-prompt production cross sections, $X(3872)/\psi(2S)$ in the single lifetime fit model [12].

non-prompt $\psi(2S)$ and $X(3872)$ are produced from the same admixture of parent b-hadrons and, therefore, implies the same lifetimes for $\psi(2S)$ and $X(3872)$ in each p_T bin. This allows determination of the ratio of the average branching fractions to be:

$$R_B^{1L} = \frac{Br(B \to X(3872)+\text{any})Br(X(3872) \to J/\psi\pi^+\pi^-)}{Br(B \to \psi(2S)+\text{any})Br(\psi(2S) \to J/\psi\pi^+\pi^-)} = (3.95 \pm 0.32(\text{stat}) \pm 0.08(\text{sys}))\%. \tag{4.2}$$

An alternative lifetime model, also implemented in this analysis, allows for two non-prompt contributions with distinctly different effective lifetimes (the "two-lifetime fit"). The non-prompt component is represented as a sum of short-lived (SL) and long-lived (LL) components:

$$F_{NP}^i(\tau) = (1 - f_{SL}^i)F_{LL}(\tau) + f_{SL}^i F_{SL}(\tau), \tag{4.3}$$

where f_{SL}^i is the fraction of SL within non-prompt. The statistical power of the data does not allow determination of two free lifetimes and so these are fixed, with f_{SL}^i left free in the fit. The LL component is assumed to originate from the usual admixture of $B^\pm$, B^0, B_s mesons and b-baryons, while any SL part would be due to the contribution of $B_c^\pm$ mesons. The lifetimes depend on the parent's lifetime and decay kinematics. The term τ_{LL} is determined from fits to $\psi(2S)$ and allows for some SL contribution, $\tau_{LL} = 1.45 \pm 0.05$ ps. The B_c decay kinematics are varied in the simulation to alter the expected SL lifetime; the mean of the variation is taken to obtain $\tau_{SL} = 0.40 \pm 0.05$ ps. The measured ratio of long-lived $X(3872)$ to long-lived $\psi(2S)$ is fitted with the kinematic template as described above, to obtain

$$R_B^{2L} = \frac{Br(B \to X(3872)+\text{any})Br(X(3872) \to J/\psi\pi^+\pi^-)}{Br(B \to \psi(2S)+\text{any})Br(\psi(2S) \to J/\psi\pi^+\pi^-)} = (3.57 \pm 0.33(\text{stat}) \pm 0.11(\text{sys}))\%. \tag{4.4}$$

This value of R_B is lower than the corresponding result from the single lifetime model, but both values are significantly smaller than the 18% expected from an estimate using Tevatron data [8] and the world average values for the branching fractions: $Br(B \to \psi(2S)) = (3.07 \pm 0.21) \times 10^{-3}$, $Br(\psi(2S) \to J/\psi\pi^+\pi^-) = (34.46 \pm 0.30)\%$ [14].

The fraction of non-prompt $X(3872)$ from short-lived sources is found to be:

PoS(DIS2017)125

$$\frac{\sigma(pp \to B_c)Br(B_c \to X(3872))}{\sigma(pp \to \text{non-prompt}\, X(3872))} = (25 \pm 13(\text{stat}) \pm 2(\text{sys}) \pm 5(\text{spin}))\%. \tag{4.5}$$

The measured differential cross section (times the relevant branching fractions) for prompt production of $\psi(2S)$ is modelled fairly well by the NLO NRQCD model [15] with long-distance matrix elements (LDMEs) determined from the Tevatron data. Similarly, the differential cross section for prompt production of $X(3872)$ is modelled well by the NLO NRQCD model when assuming the $X(3872)$ state is a mixture of $\chi_{c1}(2P) - D^0\bar{D}^{*0}$ with the $\chi_{c1}(2P)$ coupling responsible for production. In the non-prompt case, the $\psi(2S)$ differential cross section is described well by the FONLL model [16], whereas this model overshoots the data in the $X(3872)$ case and increases with p_T.

The non-prompt fractions for $\psi(2S)$ and $X(3872)$ are shown in Figure 3. In the case of $\psi(2S)$, f_{NP} increases with p_T with good agreement between ATLAS and CMS. $X(3872)$ dimuon decays show no sizeable dependence on p_T, agreeing with the CMS result obtained at $\sqrt{s} = 7$ TeV [17].

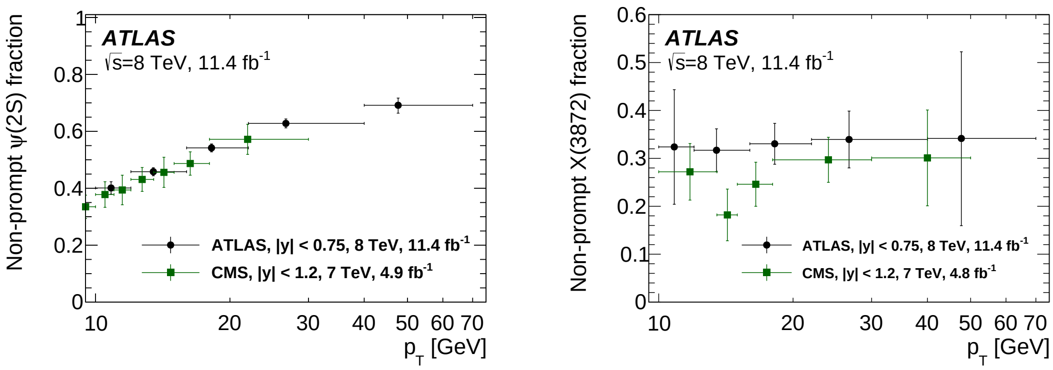

(a) (b)

Figure 3: Measured non-prompt fractions for (a) $\psi(2S)$ and (b) $X(3872)$ production compared to CMS results at $\sqrt{s} = 7$ TeV [12].

5. Dipion invariant mass spectra

The invariant mass distributions of the dipion system in the decays of $\psi(2S)$ and $X(3872)$ into $J/\psi\pi^+\pi^-$ have been measured. For $\psi(2S)$, shown in Figure 4(a) this peaks at high masses and is fitted with a Voloshin-Zakharov function:

$$\frac{1}{\Gamma}\frac{d\Gamma}{dm_{\pi\pi}} \propto (m_{\pi\pi}^2 - \lambda m_\pi^2)^2 \times \text{PS}, \tag{5.1}$$

where PS stands for the dipion phase-space. The fitted value is $\lambda = 4.16 \pm 0.06(\text{stat}) \pm 0.03(\text{syst})$, in agreement with $\lambda = 4.35 \pm 0.18$ measured by BES [18], and $\lambda = 4.46 \pm 0.25$ measured by LHCb [19]. In Figure 4(b), the normalised differential decay width of the $X(3872)$ state is shown. The shaded blue histogram is obtained from simulations, assuming the dipion system in the $X(3872) \to J/\psi\pi^+\pi^-$ is produced purely via the ρ^0 meson, and is in good agreement with the data. In both decays the $m_{\pi\pi}$ spectrum strongly disfavours the dipion phase-space distribution, shown by the red shaded area.

PoS(DIS2017)125

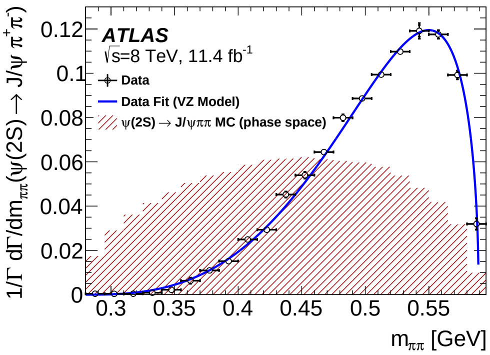

(a)

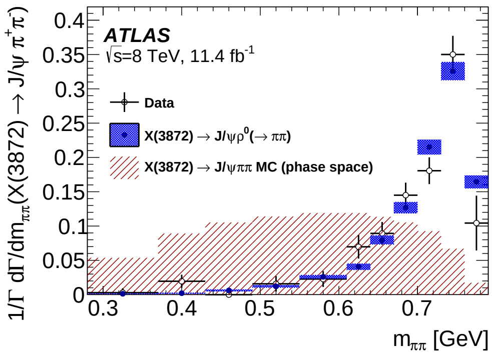

(b)

Figure 4: Normalised differential decay width as a function of invariant mass of (a) $\psi(2S)$ and (b) $X(3872)$ decays [12].

6. Summary

ATLAS has measured the hidden-charm state $X(3872)$ and $\psi(2S)$ using 11.4 fb^{-1} of $\sqrt{s} = 8$ TeV proton-proton collision data showing good agreement with the interpretation of the $X(3872)$ as a mixture of $\chi_{c1}(2P) - D^0\bar{D}^{*0}$. The measurements are consistent with similar results published by the CMS collaboration.

References

[1] Belle Collaboration, *Phys. Rev. Lett.* **91** (2003) 262001, [hep-ex/0309032].
[2] CDF Collaboration, *Phys. Rev. Lett.* **93** (2004) 072001, [hep-ex/0312021].
[3] CDF Collaboration, *Phys. Rev. Lett.* **98** (2007) 132002, [hep-ex/0612053].
[4] LHCb Collaboration, *Eur. Phys. J. C* **72** (2015) 1972, [1112.5310 [hep-ex]].
[5] LHCb Collaboration, *Phys. Rev. D* **92** (2015) 011102, [1504.06339 [hep-ex]].
[6] Tomaradze, A. *et al. Phys. Rev. Lett.* **91** (2015) 011102, [1501.01658 [hep-ex]].
[7] CMS Collaboration, *JHEP* **04** (2013) 154, [1302.3968 [hep-ex]].
[8] Artoisenet, P. and Braaten, E., *Phys. Rev. D* **81** (2010) 114018, [0911.2016 [hep-ph]].
[9] Meng, C., Han, H. and Chao, K., *X(3872) and its production at hadron colliders*, (2013), [1304.6710 [hep-ph]].
[10] ATLAS Collaboration, *JINST* **3** (2008) S08003
[11] ATLAS Collaboration, *JHEP* **09** (2014) 079, [1407.5532 [hep-ex]].
[12] ATLAS Collaboration, *JHEP* **01** (2017) 117, [1610.09303 [hep-ex]].
[13] Particle Data Group, *Chinese Physics C* **38** (2014) 090001.
[14] Particle Data Group, *Chinese Physics C* **40** (2016) 100001.
[15] ATLAS Collaboration, *Phys. Rev. D* **90** (2014) 052007, [1407.1796 [hep-ex]].
[16] Cacciari, M. *et al.*, *JHEP* **10** (2012) 137, [1205.6344 [hep-ph]].
[17] CMS Collaboration, *JHEP* **02** (2012) 011, [1111.1557 [hep-ex]].
[18] BES Collaboration, *Phys. Rev. D* **62** (2000) 032002, [hep-ex/9909038].
[19] LHCb Collaboration, *Eur. Phys. J. C* **72** (2012) 2100, [1204.1258 [hep-ex]].

PoS(DIS2017)125